Journal of Materials Chemistry B

Accepted Manuscript

ROYAL SOCIETY OF CHEMISTRY

www.rsc.org/materialsB

Journal Name

RSCPublishing

ARTICLE

Controllable Construction of Micro/nanostructured NiO in Confined Microchannels via Microfluidic Chemical Fabrication for Highly Efficient and Specific Absorption of Abundant Proteins

Cite this: DOI: 10.1039/xoxxoooooox

Received ooth January 2012,
Accepted ooth January 2012

DOI: 10.1039/xoxxoooooox

www.rsc.org/

De Zhao,‡[a] Gang Wang,‡[a] Zhongyuan He,[a] Hongzhi Wang,*[a] Qinghong Zhang[a] and Yaogang Li*[b]

Three kinds of micro/nanostructured NiO arrays were constructed in confined microchannels via a facile and template-free microfluidic chemical fabrication. Bovine serum albumin (BSA) and bovine hemoglobin (BHb) with different isoelectric points (IEPs) were chosen as the model protein to test the absorption ability of NiO-modified microchannels for abundant proteins via electrostatic interaction and affinity interaction. The influences of the pH and ionic strength of the protein solution, the residence time of protein solution in the microchannels, zeta potentials and morphologies of nickel oxide on protein absorption behavior of the modified microchannels were all studied. The NiO nanosheet arrays-modified microchannels could almost absorb all of the target protein when the protein solution (500 μg mL^{-1}) resided in the microchannnel for 120 s without separation. The excellent protein absorption ability of NiO nanosheet arrays-modified microchannels could be attributed to its high zeta potential and more absorption sites induced by the macroporous structure consisting of large nanosheets. Moreover, the NiO nanosheet arrays-modified microchannels also exhibited excellent selective absorption ability for hemoglobin from a protein mixture and human blood samples owing to the strong affinity interaction between nickel and the histidine residues of hemoglobin. Therefore, the NiO nanosheet arrays-modified microchannels showed promise for application in proteomics.

Introduction

Microfluidic technology, which is characterized by miniaturization, integration and automation, has been playing an increasingly important role in many fields such as biology separation and detection,[1] energy harvesting,[2] materials synthesis[3] and catalysis[4] etc. Among the numerous microfluidic functions, biology separation and detection is a compelling one and has been a significant research focus.[5] To date, in the bio-separation field, there are several mature methods that have been put forward, such as electrophoresis,[6] liquid chromatography[7] and magnetic separation[8] etc. These methods have shown superior separation ability in practical application. However, electrophoresis and liquid chromatography require large and expensive instruments, which not only results in high instrument costs, but also increased space costs. Compared with the former, magnetic separation is a convenient and effective method due to its excellent operability and biology separation ability. Nevertheless, magnetic separation does not allow continuous and high through-out biology separation, especially for complex clinical samples with large volumes. Additionally, the preparation of magnetic functional

[a] *State Key Laboratory for Modification of Chemical Fibers and Polymer Materials, College of Materials Science and Engineering, Donghua University, 201620 (People's Republic of China). Email: wanghz@dhu.edu.cn; Fax: +86-021-67792855; Tel: +86-021-67792881*

[b] *Engineering Research Center of Advanced Glasses Manufacturing Technology, MOE, Donghua University, 201620 (People's Republic of China). E-mail: yaogang_li@dhu.edu.cn; Fax: +86-021- 67792855; Tel: +86-021-67792526*

‡These authors contributed equally to this work.

materials is usually time-consuming and low-yield. Therefore, as a simple, rapid and efficient mean to attain ideal biology separation, microfluidic technology has attracted significant attention and seen great development.

In the bio-separation field, to improve the performance of microfluidic system, much research has focused on the modification and functionalization of the inner wall of microchannels, part of microfluidic system. By changing the chemical properties of the inner wall of microchannels, non-covalent capillary coatings, including immobilizations of small molecules,[9] surfactants[10] and other polymers,[11] has been widely used. In addition, owing to their unique micro/nanostructure and chemical properties, the construction of inorganic functional materials in microchannels has also attracted more and more attention.[12] Firstly, the introduction of micro/nanostructure is beneficial to the design and functionalization of the inner wall of microchannels. Secondly, as an important bio-separation material, inorganic functional materials should be well applied to microfluidic system to play a greater role. However, the traditional micro/nanostructures situated in microchannels are mainly constructed by high-cost, sophisticated processes such as micro-electro-mechanical system (MEMS), laser machining and ink jet printing etc. And it is impossible to construct micro/nanostructures in confined microchannels via these microfabrication processes, which leads to a complicated and time-consuming encapsulation process. Hence, chemical fabrication is a simple convenient method to construct micro/nanostructures on the inner walls of the confined microchannels. Moreover, it is worth mentioning that, under the same condition of reactants, compared with chemical fabrication in open space, microfluidic chemical fabricate on often constructs particular micro/nanostructures, due to the effects of laminar flow and confined microspace. For these reasons, microfluidic chemical synthesis should be given much more attention. We have previously demonstrated wet chemical methods to fabricate ZnO nanorods and networks on the inner walls of microchannels, which resulted in satisfactory achievement in the area of photocatalysis, protein absorption and detection.[13] Nevertheless, research work on the application of microfluidic system with inorganic functional materials on bio-separation has been limited. Therefore, it is very necessary to apply much more inorganic functional materials with micro/nanostructure to microfluidic system.

In the bio-separation field, protein absorption and separation is of great importance in key life science disciplines (e.g. diagnostics, proteomics, protein purification).[14] Serum albumin is the most abundant protein in blood plasma and has many physiological functions and can act as transporters for a variety of compounds.[15] Bovine serum albumin (BSA), as a serum albumin, has wide scale application due to its low cost, wide availability, and structural/functional similarity to human serum albumin.[16] Hence the separation of BSA is very meaningful in the biotechnology field. Because the isoelectric point of BSA is low, about 4.7, electrostatic interaction between nano-materials and protein, as a main driving force of protein absorption, has been used for the absorption and separation of BSA. Among these electrostatic absorption materials, metal compounds play an important role due to their structure controllability and good electrostatic absorption ability. The absorptions of BSA on metal compounds, such as Fe_3O_4, Al_2O_3, CeO_2, LDHs and TiO_2, via electrostatic interaction were investigated.[17] However, these functional materials don't possess extremely high or low isoelectric point, which makes them only employed in limited pH conditions, thus resulting in unstable absorption and separation effect. Furthermore, compared with non-specific protein absorption induced by electrostatic interaction, specific protein absorption has been receiving more attention. In proteomics, non-specific protein absorption and specific protein absorption could be used for the separation and depletion of abundant proteins.[18, 28] In order to develop many more types of purification materials integrating excellent non-specific with specific absorption for protein is required.

Nickel oxide, as one of the most important transition metal oxides, has received more and more attention, because of its wide applications such as catalysts,[19] lithium ion batteries,[20] super capacitor,[21] proteomics,[22] water treatment[23] and surface-enhanced raman scattering[24] etc. Because NiO has a high isoelectric point (about 11) according to the literatures,[25] it is very suitable for absorption of BSA via electrostatic interaction. However, to our knowledge, there is no reported literature regarding the absorption behavior of protein on nickel oxide via electrostatic interaction. More importantly, owing to its high affinity for histidine, nickel oxide has been serving as an important purification material for histidine-tagged protein.[22] Histidine-rich proteins play crucial roles in various physiological processes, such as cellular metal homeostasis, detoxiation, antimicrobial response and intrinsic pathway of coagulation.[26] And histidine-rich proteins have been recognized as important biomarkers for many diseases such as malaria, chronic kidney disease, and thrombotic disorders.[27]

Therefore, the separation of histidine-rich proteins from biological samples is very significant for proteomic and biomedical research. As a kind of abundant protein, bovine hemoglobin (BHb) is a typical histidine-rich protein and has 24 histidine residues on the surface, which makes it become a target object for purification.[28] However, in previous applications of biology separation, NiO was often employed in the form of powders. This method inevitably requires time-consuming volatile mixing and sample separation, so it is not suitable for continuous and high-throughput separation of protein. Thus, it is very necessary to integrate nickel oxide with microfluidic systems.

In this work, taking advantage of microfluidic chemical synthesis, we attempt to construct versatile micro/nanostructured NiO on the inner wall of microchannels using different synthesis conditions. To investigate non-specific and specific absorption ability of NiO-modified microchannels for proteins, BSA with a relatively lower isoelectric point and BHb with relatively more histidine were selected as target proteins respectively. It should be very significant and interesting to apply the micro/nanostructured nickel oxide constructed in the microchannels to highly efficient and specific absorption of abundant proteins.

Experimental

Materials

Bovine serum albumin (BSA, pI = 4.7, Mw = 66 kDa), and bovine hemoglobin (BHb, pI = 6.9, Mw = 69 kDa) were purchased from Sigma-Aldrich (St. Louis, MO, USA). Human whole blood was kindly donated by Renji Hospital (Shanghai, China). All other chemicals were of analytical grade and used without further purification. Silica glass capillaries (GL Science, Japan) with an inner diameter of 530 μm and a polyimide outer coating were used as the microchannels in this work. The inner surface of the glass capillaries was rinsed with a mixture of distilled water/concentrated sulfuric acid/peroxide (v : v : v =20 : 4 : 1, 90 43), distilled water, a mixture of distilled water/concentrated ammonia/peroxide (v : v : v =20 : 1 : 4, 90 °C) and distilled water in turn. Then the glass capillaries were dried in an oven at 80 °C.

Fabrication of micro/nanostructured NiO arrays in confined microchannels

Various micro/nanostructured NiO were constructed in the confined microchannels through a simple microfluidic chemical fabrication. The reactants adopted in this method were according to the literature.[29] Firstly, reaction solutions consisting of solution A and B were prepared. Solution A was a certain concentration of aqueous nickel sulfate solution; Solution B consisted of a certain concentration of mixed aqueous solution of potassium persulfate and aqueous ammonia; Solution A and B were drawn respectively into two syringes (10 mL) which were attached to a dual-syringe infusion pump (Model 22, Harvard Apparatus, USA) and connected by two pinheads to 'Y' pattern Teflon tubes with epoxy resin bonding in advance. Then the confined microchannels were placed in the oven at 90 °C and filled with solution as the pump drove the solutions through the 'Y' pattern teflon tubes at a set rate of 25 μL/min over a certain time. After the reaction was complete, the capillary microchannel was cleaned with distilled water. Finally, the confined microchannel was annealed at 150 °C and 300 °C for 2 h respectively.

Characterization of micro/nanostructured NiO in Confined Microchannels

The morphology of micro/nanostructured NiO was characterized by field emission scanning electron microscopy (FE-SEM, S-4800, Hitachi, Ltd., Japan). The FE-SEM samples were prepared by cutting the capillaries into pieces. The crystal structure of NiO was investigated by X-ray diffraction (XRD, D/max 2550 V, Rigaku, Japan, Cu Ka (λ = 0.154 nm) radiation at 40 kV and 200 mA in the 2θ range of 20–80 °. The XRD samples were prepared by scraping the products from the inner surfaces of capillary microchannels. Transmission electron microscopy (TEM) images, high-resolution TEM (HR-TEM) images were recorded by a JEM 2100 F (JEOL, Tokyo, Japan). The zeta potential of as-prepared NiO was measured by the Zetasizer (Nano-ZS) from Malvern Instruments.

Absorption and separation of abundant proteins (BSA and BHb) through the micro/nanostructured NiO-modified confined microchannels

Appropriate amounts of protein (BSA or BHb) were dissolved in the corresponding buffer solutions to give desired concentrations (100, 200, 500, and 1000 μg mL^{-1}) and then injected into various micro/nanostructured NiO-modified microchannels with various residence times (RT) by the injection pump. The pH of protein solution could be adjusted by the addition of NaOH or HCl; the ionic strength of protein solution could be regulated by the addition of KCl. The residence time was adjusted by changing the injecting speed of the protein solution. Determination of protein concentration at the exit was performed by the bicinchoninic acid (BCA) method using an Enhanced BCA Protein Assay. Kit (Beyotime, Jiangsu, China). After protein absorption, imidazole solution (0.1 g mL^{-1}) was injected in to the microchannels and resided for 1 h. Then PBS (30

μg mL^{-1}) was injected in to the microchannels and resided overnight to reuse.

The selectivity of NiO-modified microchannels toward proteins was investigated using the single protein solution of BHb or BSA (500 μg mL^{-1}), a protein mixture including BHb and BSA (500 μg mL^{-1} respectively) and 500-fold dilution of human whole blood. The residence time of the protein solution in the microchannels was set as 5 min. Imidazole (0.1 g mL^{-1}) was used to elute the protein absorbed on the NiO-modified microchannnels. The residence time of imidazole solution in the microchannels was set as 30 min. The UV–vis spectra of samples were obtained by a Lambda 35 ultraviolet–visible (UV–vis) absorption spectrophotometer (PerkinElmer, USA). Sodium dodecyl sulfate polyacrylamide gel electrophoresis (SDS-PAGE) was used to analyze the samples collected from the selective absorption protein process.

Results and discussion

Characterization of the micro/nanostructured NiO arrays-modified microchannels

As Fig. 1 shows, under continuous fluid construction, with two kinds of reaction solutions flowing through the microchannels, three different morphologies of NiO nanoarrays were constructed on the inner walls of the microchannels by increasing the concentration of reaction solutions, named NiO-1, NiO-2 and NiO-3 respectively.

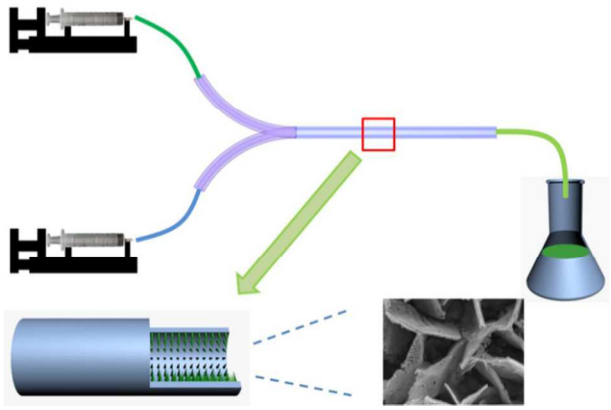

Fig. 1 Schematic diagram of the microfluidic chemical fabrication

As can be seen in Fig. 2 (a) (b), under the lowest concentration of reactants, the morphology of NiO-1 consisted of nanocluster arrays. It could be speculated that the disordered arrays were packed by generated nanoparticles with a diameter of less than 100 nm. This may be induced by the process of reactants fluid during the reaction and the low generation rate of nanoparticles.

As seen in Fig. 2 (c) (d), it was observed that the morphology of NiO-2 could be considered to be nanoflake arrays. With the increase of reactants concentration, the generation rate and stacking rate of the nanoparticles increased and the nanoflake arrays were formed finally. As shown in Fig. 2 (e) (f), under the condition of the highest concentration of reactants, there were NiO nanosheet arrays, namely NiO-3, constructed on the inner walls of microchannels. These nanosheets with a thickness of about 40 nm interconnected with each other, formed a netlike structure with macro pores with sizes of about 300-500 nm. Moreover, as shown in their respective cross-sectional views, the thickness of NiO nanoarrays increased with the increasing concentration of reacts and the thickness of NiO nanosheet arrays, namely NiO-3, was about 2.5 μm. The pores of the NiO-3 nanoarrays also possessed the highest depth, which is very beneficial for protein absorption.

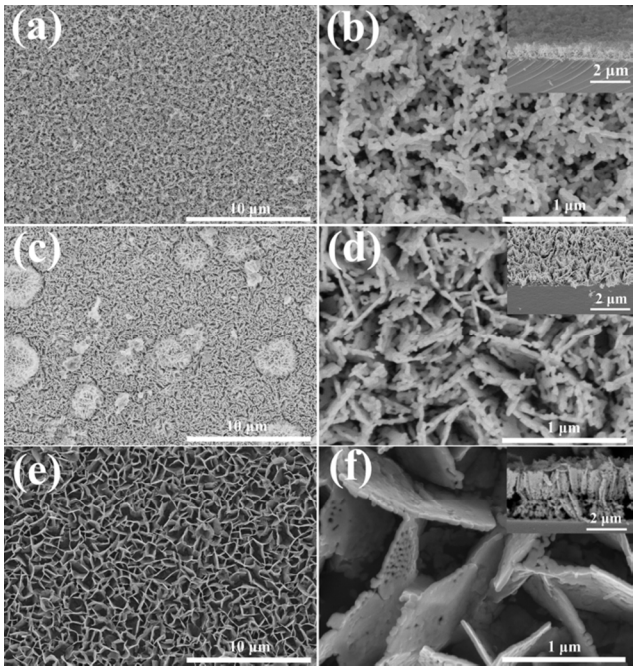

Fig. 2 FE-SEM images of the various micro/nanostructured NiO constructed in the inner surface of microchannels. (a) (b): NiO-1; (c) (d): NiO-2; (e) (f): NiO-3. The insets show the corresponding cross-sectional views.

Fig. 3 shows the XRD patterns of the as-prepared NiO scraped off the inner surface of capillary microchannels. The three diffraction peaks centered at 2-Theta angles of 37.2, 43.3 and 62.9 are observed, which can be indexed as (111), (200) and (220) crystal planes of a cubic NiO phase (JCPDS 04-0835) respectively. Moreover, it can be

clearly observed that, compared with NiO-2 and NiO-3, the crystallinity of NiO-1 was not as high, which may be a result of the lower reaction rate corresponding to the lower concentration of reactants.

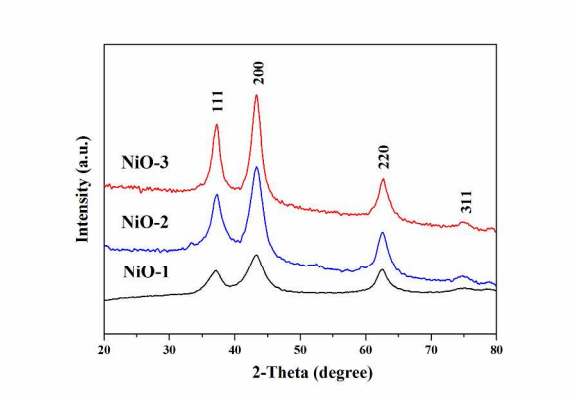

Fig. 3 XRD patterns of the as-prepared NiO scraped off the inner surface of capillary microchannels.

Fig. 4 shows the TEM and HR-TEM images of the as-synthesized NiO-3. From the TEM image, it can be seen that the NiO-3 nanoarrays consisted of many fine nanoparticles. The result is consistent with the presented FE-SEM images. The HRTEM image

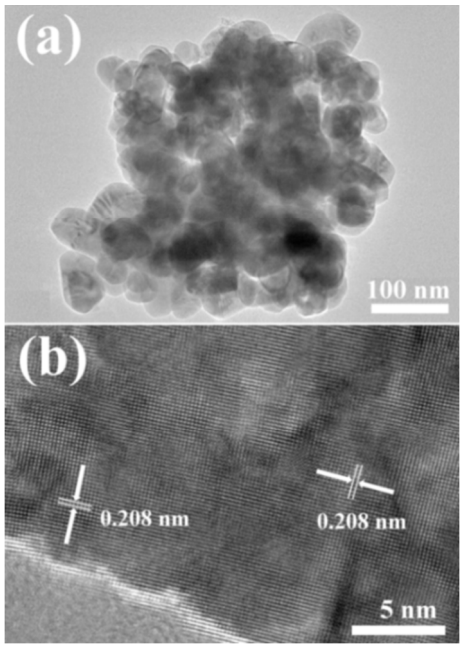

Fig. 4 (a) TEM images of the as-prepared NiO-3; (b) shows high-resolution TEM image of the as-prepared NiO-3.

shows the lattice fringes with a d-spacing of 0.208 nm, corresponding to the (220) planes of cubic NiO, which also verifies the successful preparation of nickel oxide by the microfluidic chemical method.

Nickel oxide has a high isoelectric point (IEP) of about 10.7, which makes it applicable to absorb protein by electrostatic interaction. Fig. 5 presents the zeta potentials of the as-prepared NiO as a function of pH of the buffer solution. As seen in Fig. 5, all the three kinds of micro/nanostructured NiO possessed high isoelectric point (IEP) of ~ 11, which was in accordance with the results reported in the above-mentioned literatures. However, compared with NiO-2 and NiO-3, the value of zeta potential of NiO-1 was lower. These results can be explained by the differences in crystallinity and synthesis conditions. Because nickel oxide is a p-type oxide semiconductor and has more oxygen vacancies, it has a more basic IEP. It has been reported that the defect structures have an important effect on IEPs and zeta potentials of the solid oxides and hydroxides.[30] In addition, the different synthesis conditions also lead to differences in IEPs and zeta potentials.[17c]

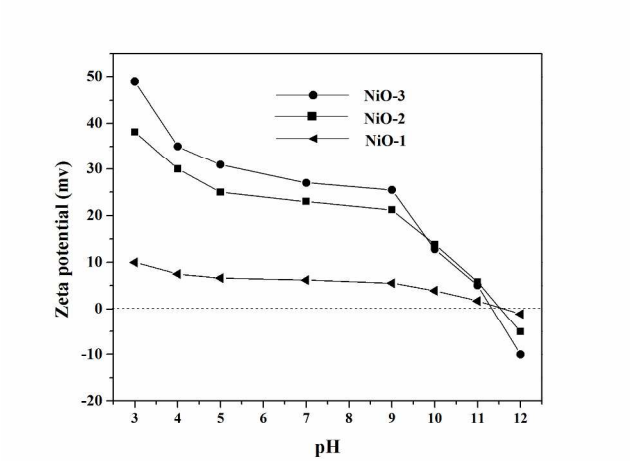

Fig. 5 Zeta-potential plots of the as-prepared NiO as a function of the pH of buffer solution.

In our work, compared with the strongly alkaline synthesis conditions of NiO-2 and NiO-3, the synthesis conditions of NiO-1 was weakly alkaline. So the synthesis condition may be the determining factors resulting in the difference in zeta potential. To further investigate the relationships between the crystallinity of nickel oxide and its zeta potentials, the as-prepared NiO were calcined in air at 500 °C for 2 h and then taken for zeta potential measurement in buffer solution. In Fig. S1, we can see that all the as-prepared NiO samples possess almost uniform crystallinity. Furthermore, as seen in Fig. S2, before and after calcination at

500 °C for 2 h, the zeta potentials of nickel oxide at different pH remained essentially unchanged. These results verified that the acidity and alkalinity of synthesis conditions is an important factor affecting the zeta potentials of as-prepared NiO.

Furthermore, because the ionic strength of the buffer solution is another key factor heavily influencing the zeta potentials of materials, the zeta potentials of as-prepared NiO-3 and two model proteins under high ionic strength were investigated. As shown in Fig. 6, when the pH of the buffer solution was 7 and the concentration of KCl solution increased to 200 mM, the zeta potentials reduced sharply, approaching zero. This result is consistent with the literatures and may provide a feasible method to eliminate the non-specific absorption induced by electrostatic interaction without changing the pH.

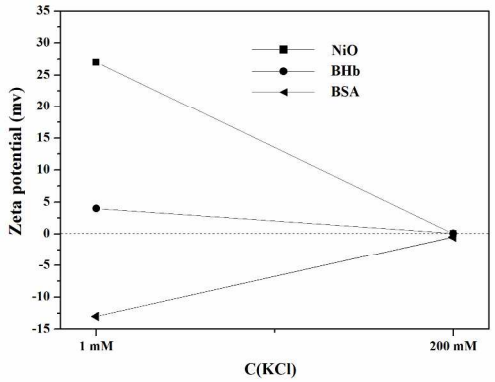

Fig. 6 Zeta-potential plots of the as-prepared NiO-3 and two proteins as a function of the concentration of KCl solution.

Non-specific and specific absorption of abundant proteins in the micro/nanostructured NiO arrays-modified microchannels

Non-specific protein absorption and specific protein absorption all can be used for the separation and depletion of abundant proteins. The electrostatic interactions and affinity interactions are the main interactions between the solid metal oxide and protein. The electrostatic interaction was identified as long-range interaction and appropriate for absorption in the microspace. In this work, BSA and BHb with dfferent IEPs were chosen as the target objects to test the absorption ability of the micro/nanostructured NiO-modified microchannels for the proteins. To confirm the IEPs of the two proteins, the plot of the zeta potentials of the two proteins as a function of pH of the buffer solution was obtained. As shown in Fig. S3, the result primarily agreed with the literature.

The pH and ionic strength of the solution greatly influence the zeta potential of NiO and protein, thereby exerting great influence on the electrostatic interaction. In this paper, under the conditions of the same ionic strength of the solution, the pH of the solution was changed to adjust the electrostatic interaction between NiO and protein. Firstly, the protein absorption behavior of as-prepared NiO-3-modified microchannnels under different pH conditions was investigated. Fig. 7 presents that the absorption capture of proteins with NiO-modified microchannels under different pH conditions in 150 s. It can be seen that the absorption capture of the proteins was greatly affected by the pH conditions. In the case of BSA, the optimum pH for the absorption was about 7. When the pH of the solution is too high or too low, the existence of the electrostatic repulsion between the nickel oxide with BSA reduces the absorption of BSA sharply. However, in the case of BHb, compared with BSA, the influence of electrostatic interaction on protein absorption was much weaker, due to the strong affinity interaction between NiO and BHb. The optimum pH for the absorption of BHb was about 9. About 60% BHb could be captured by the NiO-modified microchannels even if at pH 12.

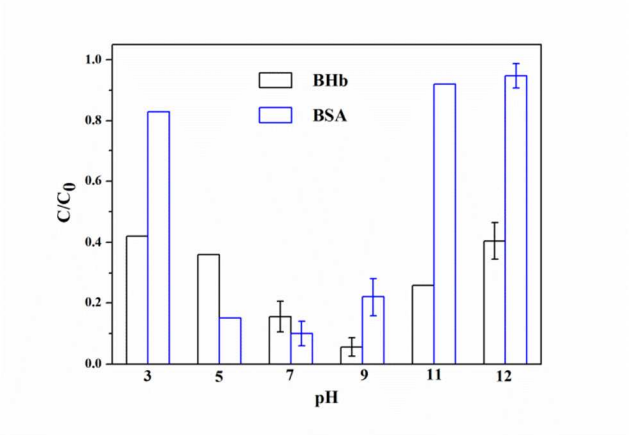

Fig. 7 Absorption capture of proteins (500 μg mL^{-1}) with NiO-3-modified microchannels under different pH conditions (C is the protein concentration at the microchannel exit, and C_0 is the concentration of target protein solution).

In addition, the protein absorption behavior of NiO-3-modified microchannels under the condition of high ionic strength was investigated. As shown in Fig. 8, in the case of BSA, when the salt concentration increased to 0.2 M, the value of C/Co increased to about 0.91 and most of the BSA was not absorbed, which indicated that the electrostatic interaction was the main driving for the absorption capture of BSA with NiO-modified microchannels; in the case of BHb, when the salt concentration was 0.2 M, the value of C/Co was also increased to 0.20, which could be caused by

competitive absorption between buffer ions and proteins. Owing to the strong affinity interaction between NiO with BHb, the modified microchannels still possessed good absorption ability for BHb.

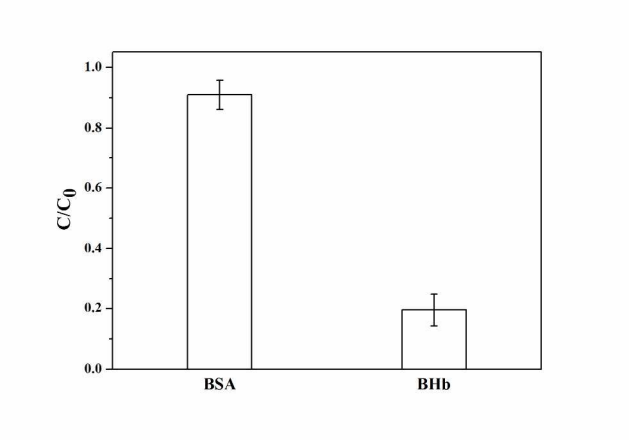

Fig. 8 Absorption capture of proteins (500 μg mL^{-1}) with NiO-3-modified microchannels at a KCl concentration of 0.2 M.

To further investigate the protein absorption behavior of the three NiO-modified microchannels, under the optimum pH, the relationship between the absorption capture of protein solution and the residence time (RT) of protein solution in the microchannel was investigated. In the case of BSA, as shown in Fig. 9 (a), all three kinds of NiO-modified microchannels possessed BSA absorption property. With increasing RT, the ratio of C to C_0 gradually decreased, suggesting that the concentration of BSA at the microchannel exit decreased. Owing to its macroporous structure consisting of large nanosheets and high zeta potential, NiO-3 exhibited the best BSA absorption property. Almost all of BSA molecules were captured by the NiO-3-modified microchannels in 120 s, while solvent molecules were flushed away through the channels. Furthermore, because electrostatic interactions was the dominant interaction between nickel oxide and BSA and the zeta potential of NiO-2 was higher than NiO-1, the NiO-2 demonstrated higher BSA absorption than NiO-1. In the case of BHb, as seen in Fig. 9 (b), a better absorption result was observed. BHb was more easily captured by the as-prepared NiO-modified microchannels than BSA. It can be speculated that the affinity interaction between nickel and BHb is the dominant driving force for BHb absorption. Likewise, the NiO-3-modified microchannel also exhibited the highest protein absorption and could capture almost all the BHb molecules in 120 s. Compared with NiO-1 and NiO-2, NiO-3 nanoarrays had a higher zeta potential and more contact sites with BHb owing to its macro porous structure consisting of large nanosheets. The whole process of protein absorption in the NiO-modified microchannel is illustrated in Fig. 10.

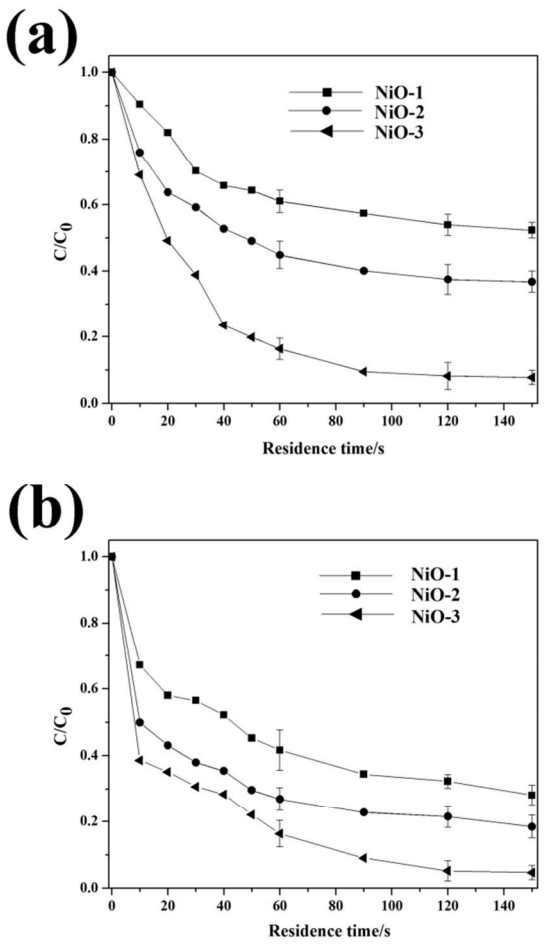

Fig. 9 Absorption capture of 500 μg mL^{-1} protein solution with various micro/nanostructured NiO-modified capillary microchannels with different RTs; (a) BSA; (b) BHb.

To further evaluate the protein absorption behavior of NiO-3-modified microchannel, different concentrations of protein were chosen as the target object to be injected to the microchannels. As presented in Fig. S4, it can be clearly seen that the two lowest concentrations, 200 μg mL^{-1} and 100 μg mL^{-1} also were almost completely absorbed in a shorter time. This shows that the NiO-modified microchannel also has good absorption ability for trace protein. However, in the case of 1000 μg mL^{-1}, only about half of the protein can be absorbed. This reveals that the modified microchannel could not absorb excessive protein in a short time, but this problem can be solved by prolonging the residence time and extending the length of the microchannel. Compared with magnetic separation, the NiO-3-modified microchannel demonstrated superior continuous

flow abundant protein absorption behavior, which can be attributed to the advantage of absorption in the microspace and the superior protein absorption ability of nickel oxide.

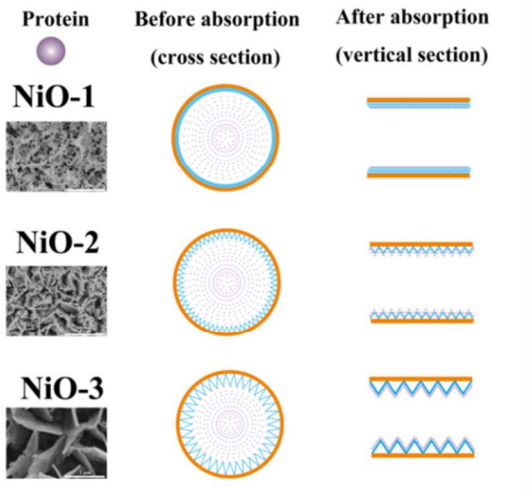

Fig. 10 Schematic diagrams of protein absorption by the three kinds of NiO-modified microchannels.

Furthermore, as shown in Fig. S5, compared with the previous ZnO nanorod-modified microchannel, the NiO-3-modified microchannels also exhibited better absorption ability for BSA and BHb. The result could be explained as follows: (1) in case of BHb, because Ni possesses much stronger affinity for histidine residues than Zn,[31] so NiO-3-modified microchannels exhibited higher protein absorption; (2) In case of BSA, because the IEP of ZnO is 9.7, lower than NiO, so NiO-3-modified microchannels also exhibited higher protein absorption at pH 7.

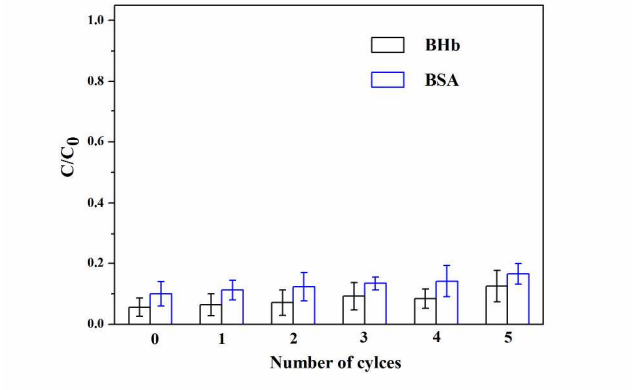

Fig. 11 Recycling performance of the NiO-3-modified microchannels used to absorb BSA and BHb with RT= 120 s. (C_0=500 μg mL^{-1}, the concentration of target protein solution; C is the protein concentration at the microchannel exit)

In addition, the recycling performance of the NiO-3-modified microchannel was investigated. As shown in Fig. 11, after five recycles, the NiO-3-modified mcrochannels could still capture over 80 % of protein molecules, which indicated that the NiO-3-modified microchannels displayed high recycling performance to capture BSA and BHb.

The above results demonstrated that NiO-3-modified microchannels possess the excellent absorption characteristics for proteins with different IEPs. However, electrostatic absorption is nonspecific and can't meet the needs of selective absorption. So it is necessary to investigative the specific absorption behavior of as-prepared NiO-modified microchannels to protein. Because of the strong affinity of nickel for histidine (His) residues, NiO is an excellent material for the purification of histidine-rich protein. As is well known, the number of accessible histidine residues on BHb is 24, while BSA has only two histidine residues on the surface. In order to achieve the selective absorption of NiO for BHb, it is necessary to avoid the non-specific protein absorption by changing pH and ionic strength.

Under high pH, electrostatic interaction could be utilized to prevent non-specific protein absorption, but it would hinder the required specific protein absorption; under high ionic strength, electrostatic interaction could be eliminated, but it could not be used to prevent the other non-specific protein absorption. Hence, the selective absorption of the modified microchannels for BHb would be performed under high pH and high ionic strength. Fig. S6 shows UV-Vis spectra of the samples obtained in absorption-desorption process of a single protein solution (BSA or BHb, 500 μg mL^{-1}) with the NiO-3-modified microchannels. As shown in Fig. S6, the characteristic absorption peaks of BHb and BSA were located at 400

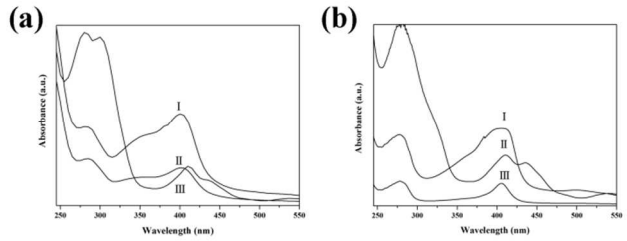

Fig. 12 UV-Vis spectra of the samples obtained in the absorption-desorption process of 500 μg mL^{-1} BHb and BSA mixture with equal mass ratio with NiO-3-modified microchannels under two different conditions. (a) 1 mM KCl, pH=12; (b) 200 mM KCl, pH=7. Curve "I" "II" "III" in the each map is the UV-Vis spectra of the samples before absorption, after absorption and after elution with 0.1 g mL^{-1} imidazole solution respectively.

nm and 285 nm respectively. From Fig. S6 (a) (b), at pH 12, it can be seen that after absorption, the intensity of the absorption peak at 285 nm and 400 nm decreased slightly and significantly, respectively, which indicated that less BSA and more BHb were absorbed; as shown in Fig. S6 (c) (d), under the high ionic strength, after treatment with the modified microchannels, compared with the absorption at high pH, the intensity of the absorption peak at 285 nm and 400 nm decreased a little more and significantly respectively, which demonstrated that more BSA and BHb were absorbed. As seen in Fig. 12, under the conditions of high pH and high ionic strength, in the absorption test of a binary solution protein mixture containing 500 μg mL^{-1} BHb and BSA, the NiO-3-modified microchannels all showed strong absorption ability for BHb and much more BHb was absorbed under high ionic strength. Because imidazole has strong metal chelating interactions with nickel, it resulted in the release of proteins from the NiO-modified microchannels. As shown in Fig. 12 and S6, BHb was released from the NiO-modified microchannels after the elution of imidazole. However, because of the presence of the imidazole and BHb in the solution, the absorption peak of BSA was not easily observed. In order to further demonstrate the selective absorption ability of NiO-modified microchannels, SDS-PAGE analysis was used to analyze the samples in the absorption test of a binary solution protein mixture.

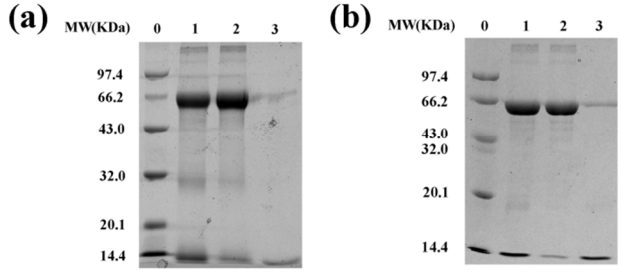

Fig. 13 SDS-PAGE analysis of the absorption of BHb by NiO-3-modified microchannels from 0.5 mg mL^{-1} BHb and BSA mixture with the equal mass ratio under two different conditions. (a) 1 mM KCl, pH=12; (b) 200 mM KCl, pH=7. Lane 0, protein molecular weight marker; Lane 1, 0.5 mg mL^{-1}BHb and BSA mixture with equal mass ratio; Lane 2, BHb and BSA mixture after treatment with NiO-3-modified microchannels; Lane 3, the absorbed protein after the elution of imidazole (0.1 g mL^{-1}).

Fig. 13 shows SDS-PAGE analysis of the protein mixture before and after treatment with NiO-3-modified microchannels. From Fig. 13 (a), under high pH, it could be observed that in lane 2, after treatment of the microchannels, the intensity of BHb faded and the intensity of BSA changed very little. In lane 3, after the elution of imidazole, the band of BHb could be also observed distinctly, but the band of BSA was hardly observed, which all demonstrated that the modified channels possess well selective absorption for BHb. As shown in Fig. 13 (b), after elution of imidazole solution, the intensity of BHb and BSA in lane 3 were all stronger than those in Fig. 13 (a) in varying degrees, which also indicated that more BHb and BSA were absorbed and the absorbed amount of BHb increased significantly more. At last, in the case of the BHb and BSA binary solution, the whole absorption process is illustrated by Fig. 14. The NiO-3-modified microchannels demonstrate fine selectively absorption for BHb under high pH and high ionic strength.

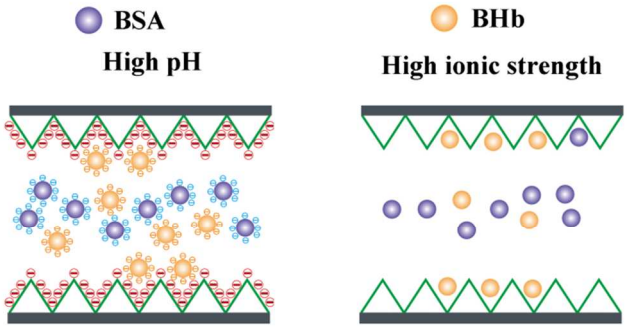

Fig. 14 Schematic diagram of the abundant proteins absorption in the NiO-3-modified microchannel under high pH and high ionic strength.

According to the previous literature, human whole blood was selected as the real sample to investigate the practicality and separation effectiveness of NiO-modified microchannels. The high

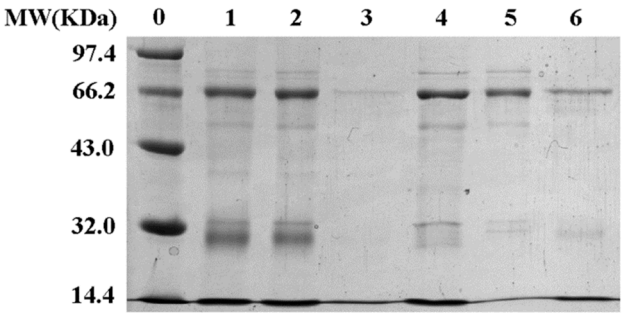

Fig. 15 SDS-PAGE analysis of human whole blood before and after treatment with NiO-3-modified microchannels under two different conditions. Lane 0, marker; Lane 1-3 were obtained unde high pH (1 mM KCl, pH=12) and Lane 4-6 were obtained under high ionic strength (200 mM KCl, pH=7) ; Lane 1(4), 500-fold human whole blood; Lane 2(5), 500-fold human whole blood after treatment with NiO-3-modified microchannels; Lane 3(6), the absorbed protein after the elution of imidazole (0.1 g mL^{-1}).

abundance of hemoglobin in biological fluid seriously hinders the detection of low abundance proteins that are often indicators for

diseases.[28d] As a typical histidine-rich protein, human hemoglobin has 24 accessible histidine residues and would be selectively depleted by the NiO-modified microchannels. In addition, the real sample would be treated by the modified microchannels under high pH and high ionic strength, so human whole blood was diluted to 500-fold by corresponding buffer solution. As shown in Fig. 15, though the modified microchannels could selectively deplete human hemoglobin under high pH and high ionic strength, the separation effects under the two conditions were different. Comparing lane 2 with lane 4, it could be seen that more human hemoglobin was absorbed by the modified microchannels under high ionic strength. In addition, the absorption of human serum under the two conditions was different. Under high pH, human serum albumin (HSA) was barely absorbed by the modified microchannel, but the absorbed amount of HSA under high ionic strength was a little higher. In conclusion, the modified microchannels could selectively absorb hemoglobin from human whole blood, demonstrating a practical application

Conclusions

Various micro/nanostructured NiO-modified microchannels with excellent protein absorption ability were successfully constructed by a simple and template-free microfluidic chemical fabrication. The NiO-modified microchannels exhibited excellent absorption ability for abundant proteins via electrostatic interactions and affinity interactions. The NiO nanosheet arrays-modified microchannel could absorb almost all target objects continuously without separation, when the protein solution (500 μg mL^{-1}) resided in the microchannel for 120 s. In addition, owing to the strong affinity between nickel and histidine residues, the NiO nanosheet arrays-modified microchannel exhibited highly selective absorption for histidine-rich protein such as hemoglobin. Owing to integrating nickel oxide into microfluidic system, besides the abundant protein absorption ability of nickel oxide, the NiO-modified microchannels have continuous and efficient operation ability of microfluidic system, which is a promising tool for highly efficient and specific absorption of abundant proteins.

Acknowledgements

We gratefully acknowledge the financial support by Natural Science Foundation of China (No. 51172042), Specialized Research Fund for the Doctoral Program of Higher Education（20110075130001）, Science and Technology Commission of Shanghai Municipality (12nm0503900, 13JC1400200), The Shanghai Natural Science Foundation (15ZR1401200), Innovative Research Team in University（IRT1221）, the Program of Introducing Talents of Discipline to Universities (No.111-2-04), and the Fundamental Research Funds for the Central Universities.

References

1 (a) A. Lenshof, T. Laurell, *Chem. Soc. Rev.*, 2010, **39**, 1203-1217; (b) S. J. Reinholt, A. J. Baeumner, *Angew. Chem. Int. Ed.*, 2014, **53**, 13988-14001; (c) A. D. Tadmor, E. A. Ottesen, J. R. Leadbetter, R. Phillips, *Science*, 2011, **333**, 58-62; (d) C. Xue, S. A. Khan, K. Yang, *Adv. Mater.,* 2009, **21**, 198-202; (e) E. K. Sackmann, A. L. Fulton, D. J. Beebe, *Nature*, 2014, **507**, 181-189.

2 (a) M. F. El-Kady, R. B. Kaner, *Nat. Commun.,* 2013, **4**, 1475; (b) T. Krupenkin, J. A. Taylor, *Nat. Commun.,* 2012, **2**, 448; (c) M. Xue, Z. Xie , L. Zhang, X. Ma, X. Wu, Y. Guo, W. Song, Z. Li, T. Cao, *Nanoscale,* 2011, **3**, 2703-2708; (d) E. Kjeang, R. Michel, D. A. Harrington, N. Djilali, D. Sinton, *J. Am. Chem. Soc.,* 2008, **130**, 4000-4006; (e) R. S. Jayashree, L. Gancs, E. R. Choban, A. Primak, D. Natarajan, L. J. Markoski , P. J. A. Kenis, *J. Am. Chem. Soc.*, 2005, **127**, 16758-16759.

3 (a) K. S. Elvira, X. C. i Solvas, R. C. R. Wootton, A. J. de Mello, *Nat. Chem.*, 2013, **5**, 905-915; (b) J. P. Luis, *Chem. Soc. Rev.,* 2014, **43**, 2253-2271; (c) A. M. Nightingale1, T. W. Phillips, J. H. Bannock, J. C. de Mello, *Nat. Commun*., 2014, 5; (d) A. N. itropoulos, G. Perotto, S. Kim, B. Marelli, D. L. Kaplan, F. G. Omenetto, *Adv. Mater.*, 2014, **26**, 1105-1110.

4 (a) S. Sengupta, D, Patra, I. O. Rivera, A. Agrawal1, S. Shklyaev, K. K. Dey, U. C. Figueroa, T. E. Mallouk, A. Sen, *Nat. Chem.*, 2014, **6**, 415-422; (b) A. DeAngelis, D. Wang, S. L. Buchwald, *Angew. Chem. Int. Ed.*, 2013, **52**, 3434-3437; (c) L. Baraban, D. Makarov, R. Streubel, I Mo¨nch, Daniel Grimm, Samuel Sanchez, O. G. Schmidt, *ACS Nano,* 2012, **6**, 3383-3389.

5 (a) J. J. Lee, K. J. Jeong, M. Hashimoto, A. H. Kwon, A. Rwei, S. A. Shankarappa, J. H. Tsui, D. S. Kohane, *Nano Lett.*, 2014, **14**, 1-5; (b) Q. Shen, L. Xu, L. Zhao, D. Wu, Y. Fan, Y. Zhou, W. H. OuYang, X. Xu, Z. Zhang, M. Song, T. Lee, M. A. Garcia, B. Xiong, S. Hou, H. R. Tseng, X. Fang, *Adv. Mater.,* 2013, **25**, 2368-2373; (c) H. Ko, J. Lee, Y. Kim, B. Lee, C. H. Jung, J. H. Choi, O. S. Kwon, K. Shin, *Adv. Mater.*, 2014, **26**, 2335-2340; (d) F. Yang , X. Zuo, Z. Li , W. Deng , J. Shi , G. Zhang, Q. Huang, S. Song, C. Fan, *Adv. Mater.*, 2014, **26**, 4671-4676; (e) F. C. Ziem, N. S. Götz, A. Zappe, S. Steinert, J. Wrachtrup, *Nano Lett.,* 2013, **13**, 4093-

4098; (f) L. Ge, S. Wang, J. Yu, N. Li, S. Ge, M. Yan, *Adv. Funct. Mater.*, 2013, **23**, 3115-3123.

6 (a) V. Poinsot, M. A. Carpéné,, J. Bouajila, P, Gavard, B. Feurer, F. Couderc, *Electrophoresis*, 2012, **33**, 14-35; (b) A. R. Timerbaev, *Chem. Rev.,* 2013, **113**, 778-812.

7 (a) K. Nanishi, N. Tanaka, *Acc. Chem. Res.*, 2007, **40**, 863-873; (b) C. Chu, R. Liu, *Chem. Soc. Rev.*, 2011, **40**, 2177-2188.

8 (a) J. Guo, W. Yang, C. Wang, *Adv. Mater.*, 2013, **25**, 5196-5214; (b) Y. Li, X. Zhang, C. Deng, *Chem. Soc. Rev.*, 2013, **42**, 8517-8539; (c) L. H. Reddy, J. L. Arias, J. Nicolas, P. Couvreur, *Chem. Rev.*, 2012, **112**, 5818-5878.

9 (a) J. S. Green, J. W. Jorgenson, *J. Chromatogr. A*, 1989, **478**, 63-70; (b) C. Gelfi, A. Vigano`, M. Ripamonti, P. G. Righetti, R. Sebastiano, A. Citterio, *Anal. Chem.*, 2001, **73**, 3862-3868.

10 (a) C. A. Lucy, A. M. MacDonald, M. D. Gulcev, *J. Chromatogr. A*, 2008, **1184**, 81-105; (b) M. D. Gulcev, C. A. Lucy, *Anal. Chem.*, 2008, **80**, 1806-1812; (c) M. D. Gulcev, T. M. McGinitie, M. F. Bahnasy, C. A. Lucy, *Analyst*, 2010, **135**, 2688–2693.

11 (a) S. Sugiura, W. Imano, T. Takagia, K. Sakai, T. Kanamori, *Biosens. Bioelectron.*, 2009, **24**, 1135-1140; (b) B. Yu, W. Cui, H. Cong, M. Jiao, P. Liu, S. Yang, *RSC Adv.*, 2013, **3**, 20010-20015; (c) R. Huang, A. R. Ferhan, L. Guo, B. Qiu, Z. Lin, D. H. Kim, G. Chen, *RSC Adv.*, 2014, **4**, 4883–4888.

12 (a) J. Seo, T. J. Lee, S. Ko, H. Yeo, S. Kim, T. Noh, S. Song, M. M. Sung, H. Lee, *Adv. Mater.*, 2012, **24**, 1975-1979; (b) E. Reátegui, N. Aceto, E. J. Lim, J. P. Sullivan, A. E. Jensen, M. Zeinali, J. M. Martel, A. J. Aranyosi, W. Li, S. Castleberry, A. Bardia , L. V. Sequist, D. A. Haber, S. Maheswaran, P. T. Hammond, M. Toner, S. L. Stott, *Adv. Mater.*, 2015, DOI: 10.1002/adma.201404677; (c) V. Krivitsky, L. C. Hsiung, A. Lichtenstein, B. Brudnik, R. Kantaev, R. Elnathan, A. Pevzner, A. Khatchtourints, F. Patolsky, *Nano Lett.*, 2012, **12**, 4748-4756; (d) H. J. Yoon, M. Kozminsky, S. Nagrath, *ACS Nano*, 2014. **8**, 1995-2017.

13 (a) H. Wang, X. Li, H. Nakamura, M. Miyazaki, H. Maeda, *Adv. Mater.,* 2002, **14**, 1662-1666; (b) X. Li, H. Wang, K. Inoue, M. Uehara, H. Nakamura, M. Miyazaki, E. Abe, H. Maeda, *Chem. Commun.*, 2003, **8**, 964-965; (c) G. Wang, G. Shi, H. Wang, Q. Zhang, Y. Li, *Adv. Funct. Mater.*, 2014, **24**, 1017-1026; (d) Z. He, Q. Zhang, Y. Li, H. Wang, *Appl. Catal. B: Environ.*, 2010, **93**, 376-382; (e) Z. He, Q. Zhang, H. Wang, Y. Li, *Biomed. Microdevices*, 2011, **13**, 865-875; (f) Q. Zhang, Q. Zhang, H. Wang, Y. Li, *J. Hazard. Mater.,* 2013, **254–255**, 318-324; (g) G. Wang, Z. He, G. Shi, H. Wang, Q. Zhang, Y. Li, *J. Colloid Interface Sci.,* 2015, **446**, 290-297.

14 (a) M. J. Taussig, O. Stoevesandt, C. A. K. Borrebaeck, A. R. Bradbury, D. Cahill, C. Cambillau, A. de Daruvar, S. Dübel, J. Eichler, R. Frank, T. J. Gibson, D. Gloriam, L. Gold, F. W. Herberg, H. Hermjakob, J. D. Hoheise, T. O. Joos, O. Kallioniemi, M. Koegl, Z. Konthur, B. Korn, E. Kremmer, S. Krobitsch, U. Landegren, S. van der Maarel, J. McCafferty, S. Muyldermans, P. Nygren, S. Palcy, A. Plückthun, B. Polic, M. Przybylski, P. Saviranta, A. Sawyer, D. J. Sherman, A. Skerra, M. Templin, M. Ueffing, M. Uhlén, *Nat. Methods*, 2007, **4**, 13-17; (b) B. Alvarez-Sanchez, F. Priego-Capote and M. D. L. de Castro, *Trends Anal. Chem.*, 2010, **29**, 120-127.

15 J. R. Simard, P. A. Zunszain, C. E. Ha, J. S. Yang, N. V. Bhagavan, I. Petitpas, S. Curry, J. A. Hamilton, *Proc. Natl. Acad. Sci. U. S. A.*, 2005, **102**, 17958-17963.

16 T. Peters, *Adv. Protein Chem.,* 1985, **37**, 161-245.

17 (a) Z.G. Peng, K. Hidajat, M.S. Uddin, *J. Colloid Interface Sci.*, 2004, **271**, 277-283; (b) K. Rezwana, L. P. Meiera, L. J. Gauckler, *Biomaterials*, 2005, **26**, 4351-4357; (c) S. Patila, A. Sandbergb, E. Heckertc, W. Selfc, S. Seal, *Biomaterials,* 2007, **28**, 4600-4607; (d) T. Zhang, Y. Zhou, M. He, Y. Zhu, X. Bu, Y. Wang, *Chem. Eng. J.,* 2013, **219**, 278-285; (e) T. Kopac, K. Bozgeyik, *Colloids Surf., B*, 2010, **76**, 265-271.

18 Y. Wang, M. Liu, L. Xie, C Fang, H. Xiong, H. Lu, *Anal. Chem.,*2014, **86**, 2057-2064.

19 J. Park, E. Kang, S. U. Son, H. M. Park, M. K. Lee, J. Kim, K. W. Kim, H. J. Noh, J. H. Park, C. J. Bae, J. G. Park, T. Hyeon, *Adv. Mater.*, 2005, **17**, 429-434.

20 Y. F. Yuan, X. H. Xia, J. B. Wu, J. L. Yang, Y. B. Chen, S. Y. Guo, *Electrochem. Commun.,* 2010, **12**, 890-893.

21 C. Wang , J. Xu , M. F. Yuen , J. Zhang , Y. Li , X. Chen, W. Zhang, *Adv. Funct. Mater.,* 2014, **24**, 6372-6380.

22 (a) I. S. Lee, N. Lee, J. Park, B. H. Kim, Y. W. Yi, T. Kim, T. K. Kim, I. H. Lee, S. R. Paik, T. Hyeon, *J. Am. Chem. Soc.,* 2006, **128**, 10658-10659;

(b) J. Kim, Y. Piao, N. Lee, Y. Park, I. H. Lee, J. H. Lee, S. R. Paik, T. Hyeon, *Adv. Mater.*, 2010, **22**, 57-60; (c) K. S. Lee, M. H. Woo, H. S. Kim, E. Y. Lee, I. S. Lee, *Chem. Commun.,* 2009, **25**, 3780-3782.

23 Z. Song, L. Chen, J. Hu, R. Richards, *Nanotechnology*, 2009, **20**, 275707.

24 Q. Zhou, G. Meng, Q. Huang, C. Zhu, H. Tang, Y. Qian, B. Chen, B. Chen, *Phys. Chem. Chem. Phys.*, 2014, **16**, 3686-3692.

25 (a) P. H. Tewari, A. B Campbell, *J. Colloid Interface Sci.*, 1976, **55**, 531-539; (b) M. Tyagi, M. Tomar, V. Gupta, *Biosens. Bioelectron.,* 2013, **41**, 110-115.

26 (a) M. Rowinska-Zyrek, D. Witkowska, S. Potocki, M. Remelli, H. Kozlowski, *New J. Chem.*, 2013, **37**, 58–70; (b) J. Zheng, Z. Lin, G. Lin, H. Yang, L. Zhang, *J. Mater. Chem. B,* 2015, **3**, 2185-2191.

27 (a) D. J. Sullivan, I. Y. Gluzman and D. E. Goldberg, *Science*, 1996, **271**, 219-222; (b) A. L. Jones, M. D. Hulett and C. R. Parish, *Immunol. Cell Biol.*, 2005, **83**, 106-118.

28 (a) M. Zhang, X. He, L. Chen, Y. Zhang, *J. Mater. Chem.*, 2010, **20**, 10696-10704; (b) G. Jian, Y. Liu, X. He,L. Chen, Y. Zhang, *Nanoscale*, 2012, **4**, 6336-6342; (c) J. Cao, X. Zhang, X. He, L. Chen, Y. Zhang, *J. Mater. Chem. B*, 2013, **1**, 3625-3632; (d) J. Zheng, Z. Lin, W. Liu, L. Wang, S. Zhao, H. Yang, L. Zhang, *J. Mater. Chem. B*, 2014, **2**, 6207-6214.

29 S.Y. Han, D. H. Lee, Y.J. Chang, S.O. Ryu, T.J. Lee, C. H. Chang, *J. Electrochem. Soc.*, 2006, **153**, C382-C386.

30 G. A. Parks, *Chem. Rev.,* 1965, **65**, 177-198.

31M. Shao, F. Ning, J. Zhao, M. Wei, D. G. Evans, X. Duan, *J. Am. Chem.Soc.*, 2012, **134**, 1071−1077